

DESIGN CHALLENGES OF A TUNABLE LASER INTERROGATOR FOR GEO-STATIONARY COMMUNICATION SATELLITES

Selwan K. Ibrahim¹, Arthur Honnibal¹, Raymond McCue¹, Michael Todd¹, John A. O'Dowd¹, David Sheils¹,
Liberis Voudouris¹, Martin Farnan¹, Andreas Hurni², Philipp Putzer², Norbert Lemke², Markus Roner²

¹FAZ Technology Ltd., 9C Beckett Way, Park West Business Park, Dublin 12, Ireland

selwan.ibrahim@faztechnology.com

²OHB System AG, Manfred-Fuchs-Straße 1, 82234 Weßling, Oberpfaffenhofen, Germany

ABSTRACT

Recently optical sensing solutions based on fiber Bragg grating (FBG) technology have been proposed for temperature monitoring in telecommunication satellite platforms with an operational life time beyond 15 years in geo-stationary orbit. Developing radiation hardened optical interrogators designed to be used with FBG sensors inscribed in radiation tolerant fibers offer the capabilities of multiplexing multiple sensors on the same fiber and reducing the overall weight by removing the copper wiring harnesses associated with electrical sensors.

Here we propose the use of a tunable laser based optical interrogator that uses a semiconductor MG-Y type laser that has no moving parts and sweeps across the C-band wavelength range providing optical power to FBG sensors and optical wavelength references such as athermal Etalons and Gas Cells to guarantee stable operation of the interrogator over its targeted life time in radiation exposed environments. The MG-Y laser was calibrated so it remains in a stable operation mode which ensures that no mode hops occur due to aging of the laser, and/or thermal or radiation effects.

The key optical components including tunable laser, references and FBGs were tested for radiation tolerances by emulating the conditions on a geo-stationary satellite including a Total Ionizing Dose (TID) radiation level of up to 100 krad for interrogator components and 25 Mrad for FBGs.

Different tunable laser control, and signal processing algorithms have been designed and developed to fit within specific available radiation hardened FPGAs to guarantee operation of a single interrogator module providing at least 1 sample per second measurement capability across >20 sensors connected to two separate optical channels.

In order to achieve the required temperature specifications of $\pm 0.5^\circ\text{C}$ across a temperature range of -20°C to $+65^\circ\text{C}$ using femtosecond inscribed FBGs (fs-FBG), a polarization switch is used to mitigate for the polarization dependent frequency shift (PDFS) induced from fs-FBG which could be in the order of > 20 pm causing $> 2^\circ\text{C}$ error in the measurement. Also special transducers were designed to isolate the strain from the FBGs to reduce any strain influence on the FBG temperature measurements while ensuring high thermal conductivity.

In this paper we demonstrate the operation of an optical FBG interrogator as part of a hybrid sensor bus (HSB) engineering model system developed in the frame of an ESA-ARTES program and is planned to be deployed as a flight demonstrator on-board the German Heinrich Hertz geo-stationary satellite.

I. INTRODUCTION

Today telecommunication satellite sensing systems require a complex wiring harness which leads to increased Assembly, Integration and Testing (AIT) effort, weight and overall cost [1-3]. Traditional point-to-point wiring of electrical temperature sensors result in the vast size and weight of the harness. The use of a hybrid sensor bus (HSB) supporting both electrical and FBG fiber optic sensors has been proposed [2] by introducing an electrical I²C sensor bus along with a tunable laser based optical interrogator that provides a flexible system which reduces the mass, volume, and complexity. The HSB system aims at telecommunication satellite platforms with an operational life time beyond 15 years in geo-stationary orbit.

Multiple temperature sensors can be implemented using FBG technology and multiplexed on a single fiber which is then connected to the fiber optics interrogator module. The light weight FBG sensors are directly inscribed in radiation tolerant fibers and mounted on a transducer which is necessary to provide decoupling of mechanical stress, but simultaneously ensuring a high thermal conductivity [3].

In the following sections we will discuss the design of the FBG optical interrogation part of the HSB system and the design measures required to ensure that optical sensing system (interrogator + sensor) deliver its required specifications over its desired operational lifetime.

II. FIBER OPTIC INTERROGATOR SYSTEM DESCRIPTION

The proposed HSB system offers a modular setup where different electrical or optical measurement modules can be plugged-in so that the maximum number of overall sensors is only limited by the number of stackable modules in the chassis. The basic HSB configuration consists of different modules which are the Power Supply Unit (PSU), the HSB Controller Module (HCM), the Interrogator Controller Module (ICM) which handles both, the electrical and optical sensor networks, the Fiber-Optic Interrogator Module Analog Front End (FIM-AFE) which is connected to the Optical Front End (OFE) assembly. For the optical fiber interrogation part, the AFE and OFE is used to interface between the fiber sensors and the FIM section of ICM.

The AFE module contains the tunable laser section which includes the modulated grating Y-branch (MG-Y) tunable laser, electronic driver circuitry and digital to analogue converters (DAC). It also includes a polarization maintaining (PM) optical isolator, PM 90:10 splitter, polarization switch, and the receiver section which includes the photodiodes, amplifiers, and analogue to digital converters (ADC) as shown in fig. 1. A Serial Peripheral Interface (SPI) is used to transfer the data between the FIM-AFE and the ICM.

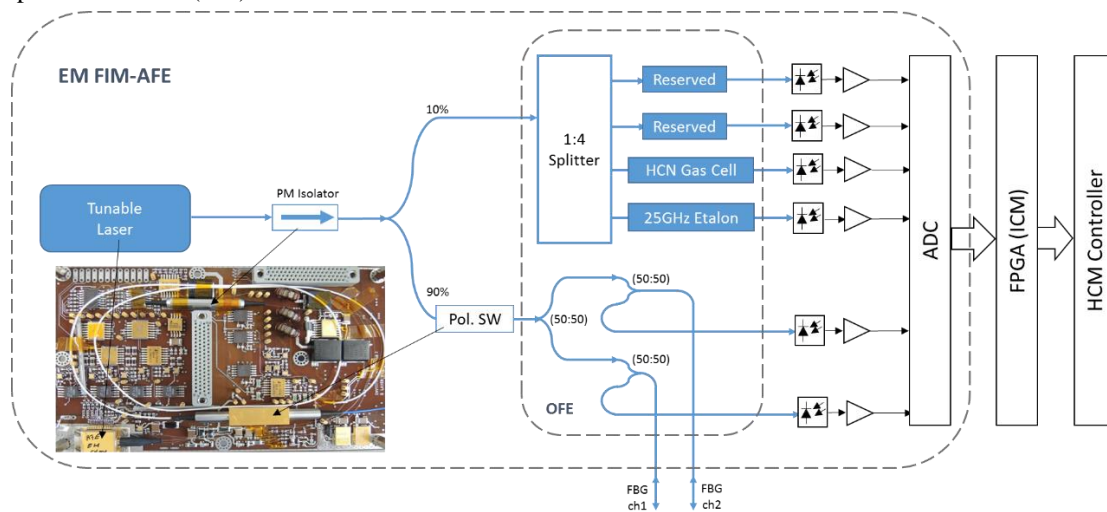


Fig. 1. Schematic diagram of the HSB Fiber Optic Interrogator Section

The MGY laser, the optical isolator and the polarization switch are mounted on the AFE PCB, which is shown in Fig 1 (left). The output of the laser after the isolator is split by a 90:10 optical coupler which provides 10% of the optical power to the reference section and the remaining 90% is used for the FBG measurement system after passing through a polarization switch. The reference section contains a passive optical splitter which provides power to an athermal Etalon which has a low finesse of about 7 and a free spectral range (FSR) of 25GHz. The Etalon is completely fiber coupled and is based internally on a free space Etalon technology. The Etalon reference is used for stitching, linearizing, wavelength correcting the sweep segments and also for the calibration, and characterisation of the tunable laser. This optical reference can also be used to detect mode jumps, and provide feedback to maintain performance over its designed lifetime of operation on both a component and/or system level. It has a sharp peak every 25GHz (200pm) which is used as a short term absolute reference in the interrogator system and is used to generate a relative frequency reference signal while the gas cell is used in the system for long term absolute referencing of the wavelength. A 100 Torr hydrogen cyanide (HCN) gas cell is used to provide stable absorption lines which are stable over temperature and radiation. The gas cell is used to correct for any long term drifts in the laser due to aging, temperature and radiation effects to guarantee stable and accurate measurements of the interrogator system. The reserved channels in the reference section shown in fig. 1 can be used to add extra optical references for improving performance, and/or providing in-situ calibration functionalities for the interrogation system. As for the FBG channels, the OFE optical assembly holds the passive optical parts such as the 3dB couplers to connect to the FBG channels and provide reflected spectra to the receiver section photodiodes. The tunable laser was calibrated to generate stable sweep segments as shown in fig. 2, which is then used to generate a quasi-continuous sweep across the C-band. The optical references are used to linearize and correct for any drifts are based on FAZ Technology's tunable laser based optical interrogators [4]. The calibrated sweep segments are stored in a look up table (LUT) in the FPGA with a wavelength resolution of 2pm. The sweep segments were generated by stepping the laser through the LUT and controlling the DAC section driving the Left/Right/Phase/SOA section currents of the MG-Y laser. The reflected spectra of the different FBG sensors are detected across the multiple fiber channels after every laser step in a synchronous fashion to reconstruct the FBG spectral shape which is then tracked using a peak detection algorithm in order to obtain a precise wavelength/temperature measurement.

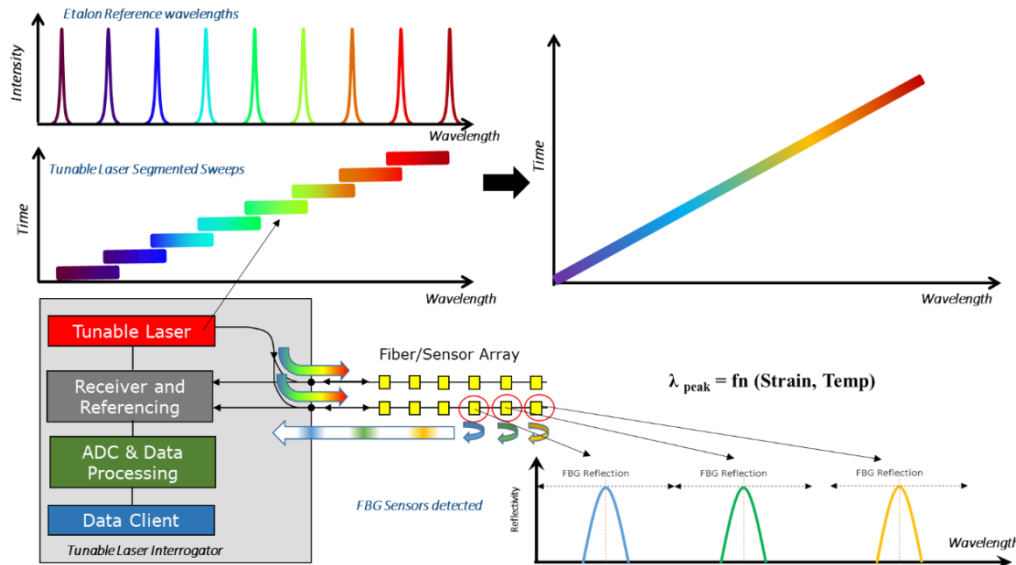


Fig. 2. Diagram of the quasi continuous sweep operation and interrogation

III. RADIATION TESTING FOR INTERROGATOR COMPONENTS

As part of the HSB system development several tests have been carried out for the critical elements in the fiber optic system. The MG-Y (Modulated-Grating Y-branch) laser was tested by subjecting it to gamma radiation and neutron displacement damage test (100krad and 1E12 neutrons/cm²) based on the worst case simulation test for a 15 year in orbit use [5]. The test results showed a shift up to 50pm after 100krad, and 1E12 neutrons/cm² on certain fixed laser output wavelength points that were set by driving the laser sections with fixed currents stored in a look up table. This confirmed that it was not sufficient to rely on a static LUT with fixed wavelengths to achieve the $\pm 5\text{pm}$ ($\pm 0.5\text{ }^\circ\text{C}$) specification for the HSB. To address this issue the calibration of the laser changed from a single LUT with a table of fixed wavelengths to a LUT containing information to sweep over multiple overlapping sweep segments. In addition to using the athermal Etalon, a HCN 100Torr gas cell was used in the system as an absolute reference that provides absolute wavelength markers (gas absorption lines) for correcting any long term drifts in the system by the laser and Etalon. Both the Etalon and gas cell reference were also subjected to similar radiation levels to those experienced by the laser in order to measure its performance in expected radiation environments. The radiation testing setup used the FAZT Technology high precision interrogator (FAZT V4) with a tunable laser light source, and a receiver board to acquire the data of the four optical components under test. The FAZT V4 instrument has four optical channels connected to circulators and then to each optical component under test to allow the system to operate in reflection mode. The Etalon and Gas Cell were connected to 2 of the V4 channels and were monitored during the radiation tests. Fig. 3 shows a photo of the radiation test set-up at Fraunhofer INT in Euskirchen, Germany.

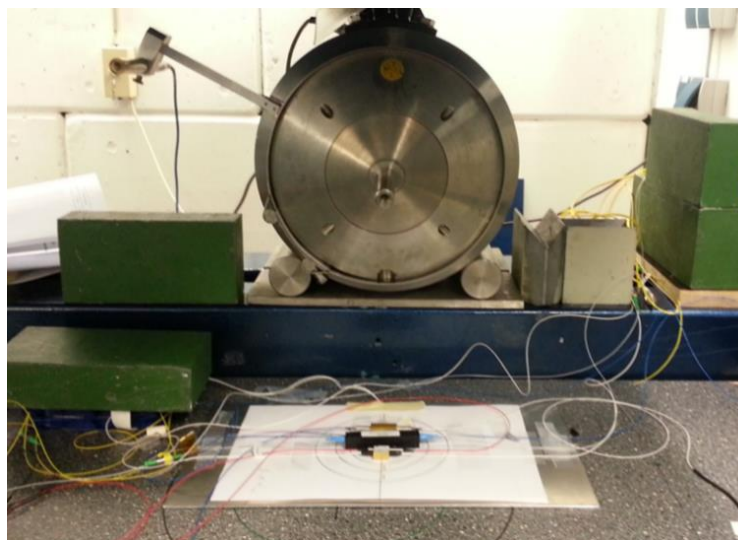


Fig. 3. Photo of Radiation test set-up at Fraunhofer INT

The Total Ionization Dose (TID) dependence of test time is shown below in Fig. 4. There were two steps in the Gamma radiation testing; in the first step for the first two hours the dose rate was set to 5 krad/hr with a total TID of 10krad, the second step of the testing increased the dose to 20 krad/h for a period of four and a half hours until 100 krad was reached.

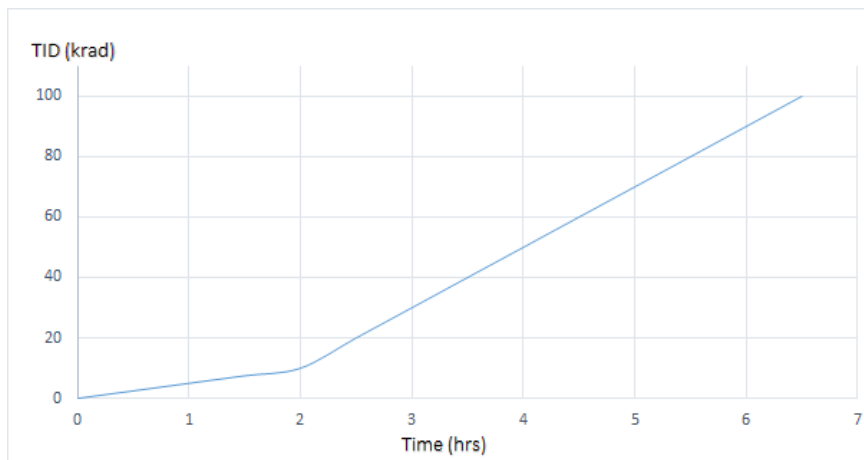


Fig. 4. Total Ionization Dose (TID) vs. the test time

The duration of the gamma radiation test was 6.5 hours and all the tests were completed within one day. At the end of the day, during the night the gamma source was switched off, but the acquisition units continuously monitored the components in order to measure annealing effects for a further 10 hours.

Throughout the Gamma Radiation test stages both the temperature within the radiation chamber and the DUT's were continuously monitored. There were two PT100 thermocouples, one placed within the chamber to measure room temperature, and a second thermocouple placed beside the DUT's to measure the temperature experienced by the DUT's throughout the test stages.

Fig. 5 shows the spectral response for all the 100Torr HCN Gas Cell absorption lines across the C-band (left), measured with the FAZT V4 interrogator at different dose rates and a zoomed in view of the spectral response of the absorption lines P Branch 06, P Branch 07, and P Branch 08 (right). The Gas cells are precision filters whose absorption lines are determined by molecular energy levels. Hydrogen Cyanide gas absorption has been widely researched and identified by national standards bodies as a primary wavelength reference in the band 1525nm to 1565nm. The gas cells are NIST traceable, have unparalleled accuracy, and have extremely low drift. Standard pressures offered are 100 Torr matching the NIST SRM2517. The absorption lines are constant over temperature, so the gas cell can be used as an absolute reference feedback signal.

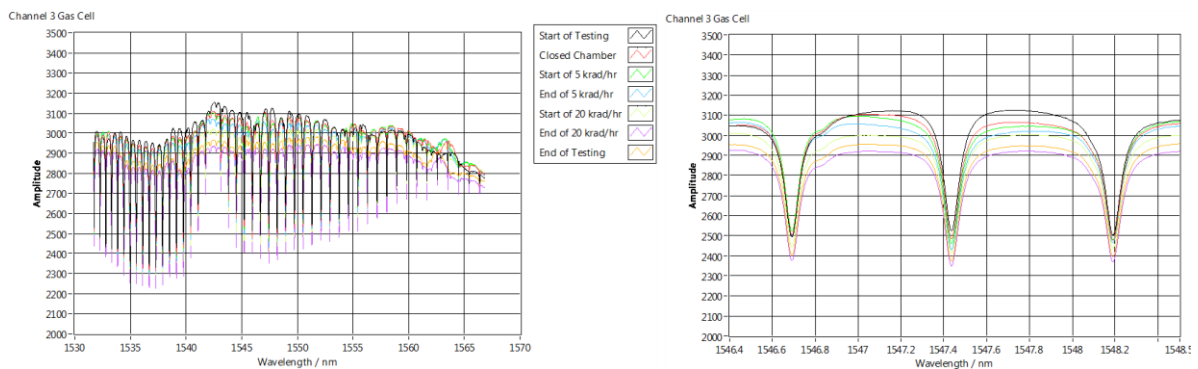


Fig. 5. Overall Spectral Response of the Gas Cell Lines in the C-band (left), Zoomed in for absorption lines P Branch 06, P Branch 07, and P Branch 08 (right)

Below in Table 1 is the mean absorption line during each stage of the radiation testing, compared to the settled absorption line measurement when the chamber was closed (start of test, or baseline of absorption line before test started). The table also shows a peak location difference from the measured absorption line during each test to the baseline measurement when the chamber was closed. The results show a maximum change of 0.32pm for the worst absorption line throughout all the radiation test stages.

Table 1. HCN Gas Cell Line Results over all stages

Chamber Closed (pm) Before Test Started	During 5krad/hr (pm)	Difference (pm)	After 5krad/hr (pm)	Difference (pm)	During 20krad/hr (pm)	Difference (pm)	After 20krad/hr (pm)	Difference (pm)
1534971.90	1534971.88	-0.02	1534971.86	-0.05	1534971.82	-0.08	1534971.74	-0.16
1535538.91	1535538.89	-0.02	1535538.87	-0.05	1535538.85	-0.06	1535538.84	-0.07
1536115.62	1536115.61	-0.01	1536115.61	-0.01	1536115.60	-0.02	1536115.59	-0.03
1546689.96	1546690.16	0.20	1546690.28	0.32	1546690.27	0.31	1546690.22	0.26
1547436.17	1547436.12	-0.05	1547435.92	-0.25	1547435.89	-0.28	1547435.92	-0.25
1548189.17	1548189.09	-0.08	1548189.23	0.06	1548189.24	0.07	1548189.17	0.00

Figure 6 (left) shows the full spectral response of a 25GHz athermal Etalon where the 3 sweep segments of 3 peaks are continuously monitored throughout the tests (highlighted in red) and were selected to cover different parts of the full C-band (Etalon 1, 2, 3, 4, 5, 6, 7, 8, 9 : 1532.08nm, 1532.28nm, 1532.48nm, 1548.3nm, 1548.5nm, 1548.7nm, 1565.9nm, 1566.1nm, 1566.3nm). Figure 6 (right) shows an example of 3 neighboring peaks within a sweep segment tracked throughout the test. The Etalon is specified to have a 25 GHz FSR (Free Spectral Range) between peak to peak, whereby 1 GHz is equivalent to ~8pm, therefore the spacing between neighboring peaks is ~200pm. It has a sharp peak every 25GHz which is used as an absolute reference (short term absolute reference) in the interrogator system. This optical reference can also be used to detect mode jumps, and provide feedback to maintain performance over its designed lifetime of operation on both a component and/ or system level.

The main part of this test is to ensure that the spacing between each neighboring peak are kept constant throughout the tests at 25GHz (200pm). The peaks were also individually tracked to determine any shift in the Etalon peaks through radiation effects or thermal effects. Throughout the Gamma Radiation test any change in the attenuation, a shift in absolute wavelength, change in FSR, or any change in spectral response of the 9 selected Etalon peaks are monitored.

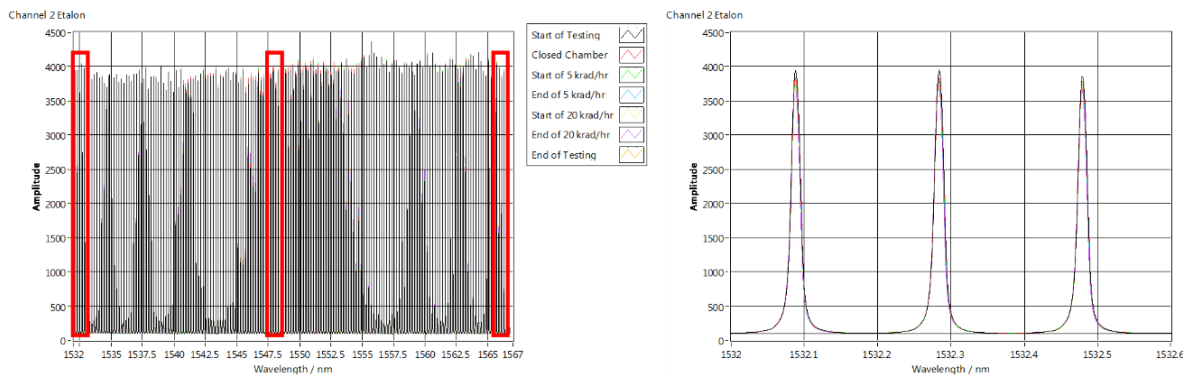


Fig. 6. Etalon Filter 25GHz Peaks across the full C-band (left), zoomed in around 3 Etalon peaks 25GHz spaced (1532.08nm, 1532.28nm, 1532.48nm) (right)

Below in Table 2 is the mean spacing between Etalon peaks throughout all the radiation test stages. The results are calculated in 3 separate segments; segment 1 (Etalon peaks 1 to 3), segment 2 (Etalon peaks 4 to 6), and segment 3 (Etalon peaks 7 to 9). Each segment has neighboring Etalon peaks, in which they are spaced 25 GHz (~200pm). The results show that all the spacings between neighboring Etalon peaks remain at 200pm throughout the test with a standard deviation (Std) of < 0.06pm.

Table 2. Measured spacing between Etalon Peaks in pico-meters

Etalon Peak Difference	Pico-meter (pm) Wavelength Spacing Between Etalon Peaks											
	Chamber Open		Chamber Closed		During 5krad/hr		After 5krad/hr		During 20krad/hr		After 20krad/hr	
	Mean	Std	Mean	Std	Mean	Std	Mean	Std	Mean	Std	Mean	Std
Etalon 1-2	199.83	0.05	199.84	0.05	199.81	0.04	199.82	0.05	199.84	0.05	199.83	0.05
Etalon 2-3	199.97	0.05	199.94	0.04	199.96	0.04	199.98	0.05	199.98	0.05	200.02	0.05
Etalon 4-5	199.91	0.05	199.95	0.05	199.92	0.05	199.91	0.05	199.88	0.05	199.88	0.05
Etalon 5-6	199.81	0.04	199.80	0.05	199.79	0.04	199.78	0.05	199.81	0.05	199.81	0.05
Etalon 7-8	199.93	0.06	199.95	0.05	199.93	0.05	199.90	0.06	199.90	0.05	199.86	0.06
Etalon 8-9	200.07	0.06	200.05	0.05	200.04	0.05	200.05	0.06	200.04	0.06	200.08	0.06

In addition to the radiation tests for the key critical components of the system (Tunable Laser and Etalon), they were also tested and validated for use in a launcher environment by subjecting them to extreme temperature and vibration tests as was reported in [6]. The vibration tests included resonance tests up to 2.5g, sinusoidal tests up to 22.5g, and random vibration tests up to 20g all over 3-axis within a 5-2000Hz frequency range, while the thermal tests covered an operating range from -20°C to +70°C. The environmental tests proved that the components may be used before, during and after a launcher take-off [6].

V. SENSOR TESTING

In addition to testing the key components of the interrogator, the FBG sensors and fibers were tested for their tolerance to radiation and environmental effects. A detailed review of radiation effects in FBG sensors and in optical fibers was reported in [3] showing the possibility to survive an extremely high total ionizing (TID) dose up to 25 Mrad which makes it possible to mount the sensors outside of the satellite. Femto-second inscribed FBGs (fs-FBG) were selected as the sensor candidate to be used in the temperature transducer due to their compatibility with radiation tolerant fibers. The radiation tests shows that attenuation in the fiber and change in reflectivity were at acceptable levels, however improvements needs to be made on the wavelength induced shift on the FBG. In order to evaluate the wavelength shift due to radiation exposure, other effects that also induce wavelength shifts in the FBG peak should be isolated such as polarization dependent frequency shift (PDFS) where $>30\text{pm}$ ($>3^\circ\text{C}$ temperature error) in certain type of fs-FBGs has been reported [7].

Here we evaluate the PDFS of two fs-FBG samples manufactured by Fraunhofer IOF institute in Jena, Germany for the project. Fig. 7 shows the spectral response of two sample fs-FBGs (FBG1@1548.872nm, and FBG2@1548.504nm center wavelengths) measured at lab room temperature. The fs-FBGs had a grating period of 537.5nm, reflectivity of $\sim 55\%$, and full width half maximum (FWHM) of $\sim 0.35\text{nm}$. The FAZ I4 interrogator system has a polarization switch which was used to evaluate the PDFS of the two fs-FBG samples [7]. The I4 interrogator was scanning @1kHz sweep rate and the pol SW was turned ON while tracking the fs-FBG peaks at room temperature.

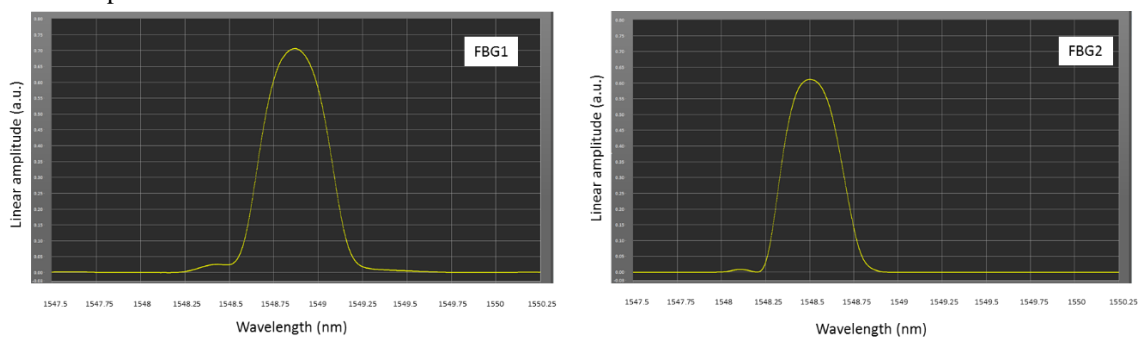


Fig. 7. Spectral response of two fs-FBG samples connected to two FAZ I4 interrogator channels

Fig 8. (left) shows the fs-FBG peak (FBG1) tracked on Ch1 (Pol SW ON, peak tracking at 1kHz) where the measured PDFS (peak-to-peak) was measured to be $\sim 18.5\text{pm}$ without averaging or mitigation. When enabling the polarization mitigation (Pol SW ON) and a moving point average (MPA) of 2 was used for averaging the PDFS p-p was reduced to $\sim 1.75\text{pm}$. Fig. 8 (right) shows the fs-FBG peak (FBG2) tracked on Ch2 (Pol SW ON, peak tracking at 1kHz) where the measured PDFS p-p was measured to be $\sim 13.5\text{pm}$ without averaging/mitigation. When enabling the polarization mitigation (Pol SW ON and MPA of 2 was used for averaging the PDFS p-p was reduced to $\sim 1.2\text{pm}$.

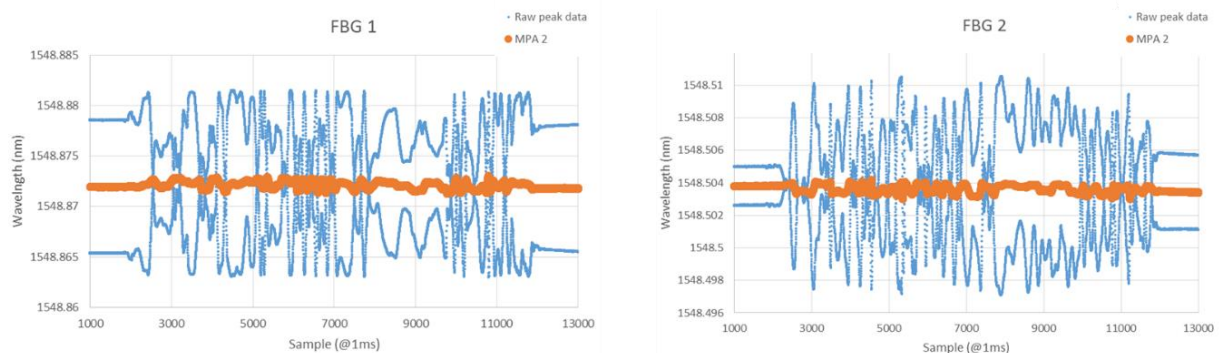


Fig. 8. FBG1 on Ch1 with Pol SW ON and peak tracking at 1 kHz (left), FBG2 on Ch1 with Pol SW ON and peak tracking at 1 kHz (right)

The FBGs were also packaged in special transducers in order to isolate the strain effects from the temperature measurements as reported in [3].

VI. INTERROGATOR DEMONSTRATOR

The HSB system was designed to measure temperature within $\pm 0.5^\circ\text{C}$ accuracy across a temperature range of -20°C to $+65^\circ\text{C}$. Here we demonstrate that this accuracy was achievable by testing the proposed interrogator system with a calibrated commercial optical FBG sensor from Lakeshore which was designed to operate from -200°C to $+250^\circ\text{C}$. For these tests two lakeshore FBG sensors were connected in series on a single fiber. The wavelength of the first sensor was $\sim 1545\text{nm}$ (#2631), while the other was at $\sim 1548\text{nm}$ (#2634). The FWHM of both sensors were $\sim 250\text{pm}$. A second order polynomial was used as a calibration function to convert the wavelength values to temperature. The coefficients were calculated from a separate calibration test that generated a look up table showing the different wavelengths measured at different temperature set points from -30°C to $+100^\circ\text{C}$ using the FAZ I4 interrogator. The HSB FIM optical interrogator was configured to sweep at $\sim 0.7\text{Hz}$ over a wide 40.75nm range (1527.50nm - 1568.25nm) with the polarization switch active, to average the two orthogonal polarization states to mitigate for PDFS effects. The sensors were placed in a thermal chamber and the temperature of the chamber was ramped from -30°C to $+70^\circ\text{C}$ and back to -30°C in 20°C steps. The wavelength shift of the two lakeshore sensors are shown in fig. 9 (left). The chamber was deemed to have reached its target temperature when it was within $\pm 0.5^\circ\text{C}$ of the target temperature for 5 consecutive minutes. After this point the chamber remained at this equilibrium temperature for an additional 90 minutes. A 2nd order polynomial coefficients were applied to each measurement point to calculate the corresponding temperature as shown in fig. 9 (right).

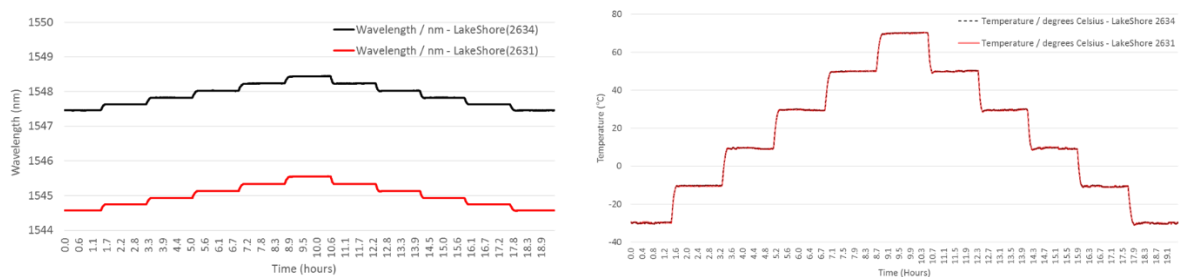


Fig. 9. Wavelength shift of the two Lakeshore sensors when temperature cycled from $-30^\circ\text{C} \rightarrow +70^\circ\text{C} \rightarrow -30^\circ\text{C}$ in 20°C steps (left), Temperature measurements after applying 2nd order conversion formula (right)

Table 3 shows the mean value for the last 5 minutes data points at each temperature steps and the offset from the thermal chamber set temperature which indicates the max error in the temperature measurement. The max offset from the oven set temperature was $<0.76^\circ\text{C}$ which could be due to the oven stability/accuracy of $\pm 0.5^\circ\text{C}$.

Table 3. Mean value of Lakeshore measured temperature and offset from oven set temperature

Set Temperature (°C)	Lakeshore (#2631) Mean Temp (°C)	Offset from Set Temperature (°C)	Lakeshore (#2634) Mean Temp (°C)	Offset from Set Temperature (°C)
-30	-29.5977	-0.4023	-29.6196	-0.3804
-10	-10.4512	0.4512	-10.2199	0.2199
10	9.36552	0.63448	9.38307	0.61693
30	29.5806	0.4194	29.672	0.328
50	49.9161	0.0839	49.9533	0.0467
70	70.0269	-0.0269	70.1541	-0.1541
50	49.9288	0.0712	50.0393	-0.0393
30	29.4936	0.5064	29.6307	0.3693
10	9.42949	0.57051	9.38622	0.61378
-10	-10.7599	0.7599	-10.6658	0.6658
-30	-30.0566	0.0566	-30.0724	0.0724

The HSB FIM optical interrogator system was also designed to support >20 sensors @ 1Hz sample rate. The architecture was implemented to support up to 32 sensors across the two channels. However, for the target application for the HSB system, 16 temperature sensors (2 arrays of 8 FBG sensors) captured at 1Hz was required. Fig. 10 shows the tracking of 16 FBG sensors distributed across the two channels (8 per channel) captured at 1Hz highlighting the stability of the system for $\sim 4.8\text{hours}$ showing the stability operation of the system. The polarization switch was active during the full duration and the wavelength scan range was $\sim 27.7\text{nm}$

which was sufficient to fit the 8 sensors/channel. It is also possible to increase the wavelength scan range to 35nm at 1Hz sweep rate by increasing the step size of the laser and/or optimizing the capture code in the FPGA. Two of the FBG sensors (FBG1, FBG2) that were connected on channel #1, were fs-FBGs and were mounted in a transducer package similar to that reported in [3].

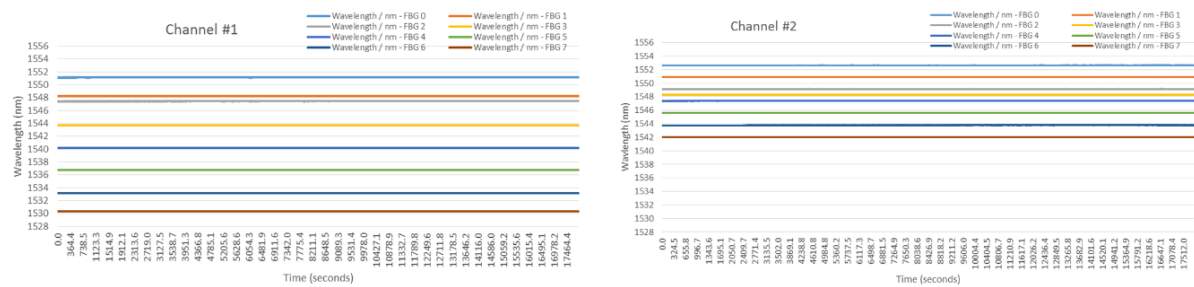


Fig. 10. Tracking of a total of 16 FBG sensors @ 1Hz for ~4.8 hours with 8 sensors on channel#1(left) and 8 on channel#2 (right)

VII. CONCLUSION

The design and operation a fiber optic interrogator system as part of a hybrid sensor bus system (HSB) engineering model has been demonstrated with 16 FBG sensors scanned at 1Hz. A polarization mitigation technique using a polarization switch was also introduced in the system to achieve the desired specifications of $\pm 0.5\text{pm}$ ($\sim\pm 0.5^\circ\text{C}$) using radiation tolerant femto-second inscribed FBGs (fs-FBG). The performance of the system was also evaluated using commercial FBG temperatures sensors operating from -30°C \rightarrow $+70^\circ\text{C}$. The HSB system is planned to be used as a flight demonstrator on-board the German Heinrich Hertz geo-stationary satellite.

VIII. ACKNOWLEDGEMENT

The Hybrid Sensor Bus Fiber optic interrogator activity is co-funded by ESA ARTES 5.2 Telecom-Technology programme under contract no. 4000104262/11/NL/US. The authors would like to thank King Lam and Iain McKenzie from the ESA for their open and productive discussions.

REFERENCES

- [1] I. Mckenzie, and N. Karafolas, "Fiber optic sensing in space structures: the experience of the European Space Agency," *In Proc. 17th International Conference on Optical Fibre Sensors*, SPIE 5855, pp. 262-269, 2005.
- [2] A. Hurni, N. M. K. Lemke, M. Roner, J. Obermaier, P. Putzer, N. Kuhenuri Chami. "Fiber-Optical Sensing On-Board Communication Satellites," *In Proc. International Conference on Space Optics ICSO 2014*, 2014.
- [3] P. Putzer, N. Kuhenuri, A. W. Koch, A. Hurni, M. Roner, N. Lemke, "Selection of fiber-optical components for temperature measurement for satellite applications," *In Proc. International Conference on Space Optics ICSO 2014*, 2014.
- [4] S.K. Ibrahim, M. Farnan, D.M. Karabacak, J.M. Singer, "Enabling technologies for fiber optic sensing," *SPIE Photonics Europe 2016*, Proc. SPIE 9899, paper 98990Z, 2016.
- [5] M.Roner, P. Putzer, A. Hurni, S. Schweyer, N. Lemke, "Total Ionizing Dose and Displacement Damage Effects in a Tunable Laser Diode Based Fiber Optic Sensing System." *In 15th European Conference on Radiation and Its Effects on Components and Systems (RADECS)*, pp. 1-5, 2015.
- [6] S.K. Ibrahim, J. O'Dowd, R. McCue, A. Honniball, and M. Farnan, "Design Challenges of a High Speed Tunable Laser Interrogator for Future Spacecraft Health Monitoring," *CLEO 2015: Applications and Technology*, ATu1M-3, 2015.
- [7] S. K. Ibrahim, J. Van Roosbroeck, J. O'Dowd, B. Van Hoe, E. Lindner, J. Vlekken, M. Farnan, D. M. Karabacak, J. M. Singer, "Interrogation and mitigation of polarization effects for standard and birefringent FBGs," *In SPIE Commercial+ Scientific Sensing and Imaging*, paper 98520H, 2016.